Effects of wave exposure on circulation in a temperate reef environment

Graham Symonds, Liejun Zhong and Nick A. Mortimer

Centre for Australian Weather and Climate Research-A partnership between CSIRO and the Bureau of Meteorology

CSIRO Wealth from Oceans Flagship, Floreat, Western Australia

ABSTRACT

Observations of waves and currents in a temperate reef environment off southwestern Western Australia over a period of one year reveal the relative importance of wind and wave forcing. During periods of low waves linear regression analysis shows alongshore currents seaward and shoreward of the reef line are reasonably well predicted using 1% and 0.5% of the wind speed respectively. However, shoreward of the reef line anomalously strong currents were often observed during periods of light or even opposing winds and the mean sea surface was elevated relative to offshore of the reefs. These anomalous currents and elevated sea level occur during periods of high waves and both are correlated with the root-mean-square wave height seawards of the reefs, similar to what has been observed in coral reef environments. The observations were simulated with the numerical model XBeach which includes radiation stress forcing due to the presence of the waves. The model was also used to examine the dynamics of the wave driven flow in terms of the momentum balance. As on a coral reef, through the surf zone over the reef bottom friction is balanced by the sum of the radiation stress gradient and pressure gradient. Away from the reefs the radiation stress gradients are small and the momentum balance is between bottom friction and pressure gradient.

1. INTRODUCTION

Coastal waters off South West Western Australia are unusual, supporting high benthic biomass and a winter phytoplankton bloom, while the pole-ward flowing Leeuwin Current is nutrient poor [*Koslow et al*, 2008]. The region is micro-tidal, dominated by diurnal tides with a spring range of about 0.7m, exposed to long period southern ocean swell (8s<T<20s), and a strong sea-breeze cycle during summer months. A feature of the coastal zone is a series of limestone reefs dotted along the coast for about 700km between 3-10km offshore [*Pattiaratchi et al*, 1995]. The distribution of the reefs is very patchy, individual reefs have relatively small areal extent and the depth over the reef crests is quite variable such that the onset of wave breaking varies from one reef to another. The level of exposure to waves is thought to have a significant impact on benthic communities on and around the reefs [*Phillips et al*, 1997; *Wernberg and Thomsen*, 2005; *England et al*, 2008].

Mean currents on the inner shelf off South West Western Australia, inshore of the Leeuwin Current but offshore of the reefs, are largely wind driven [*Pattiaratchi et al*, 1995; *Zaker et al*, 2007] and *Feng et al* [2006] report the alongshore current at 20m depth is 2.5-3% of the wind speed with a correlation of .87. In the lagoon, shoreward of the reefs, the correlation between wind and current is less and *Pattiaratchi et al* [1995] report periods during winter months when the current and wind are in opposing directions. *Zaker et al* [2007], using the same data described by *Pattiaratchi et al* [1995] report the currents inside the lagoon are dominated by wind forcing for most of the year. However, breaking waves have the potential to drive strong currents over the shallow reefs [*Symonds et al*, 1995] and, during high wave events, the wave-driven currents may dominate over wind forced currents. These cross-reef currents are due to a body force associated with gradients in the radiation stress defined as the excess momentum due to the presence of the waves [*Longuet-Higgins and Stewart*, 1964]. Due to the greater mass under the wave crest, relative to the trough, the depth integrated forward momentum flux under the wave crest is greater than the opposite momentum flux under the trough.

Averaged over a wavelength there is a net flux of momentum in the direction of the waves known as radiation stress and is proportional to wave energy [*Longuet-Higgins and Stewart*, 1964]. Horizontal gradients in radiation stress, due to gradients in wave energy, cause a body force which on a beach can force alongshore currents [*Bowen*, 1969; *Longuet-Higgins, 1970a,b*; *Thornton and Guza*, 1986] and cross-shore setup [*Bowen et al*, 1968; *Guza and Thornton*, 1981]. In the latter case the shoreline prevents any cross-shore flow, resulting in an increase in sea surface elevation at the shoreline, known as wave setup, such that the cross-shore gradient in radiation stress is balanced by an offshore directed pressure gradient. In the presence of wave breaking on a shallow reef, cross-reef currents can also result since, unlike a beach, there is no shoreline to constrain the flow or support wave setup [*Symonds et al*, 1995].

These wave forced mean flows are known to be important on coral reefs [Roberts and Suhayda, 1983; *Kraines et al*, 1998; *Kraines et al*, 1999; *Tartinville and Rancher*, 2000; *Callaghan et al*, 2006; *Monismith*, 2007; *Lowe et al*, 2009] and can have a significant impact on nutrient uptake in coral communities [*Atkinson et al*, 1994; *Bilger and Atkinson*, 1992; *Atkinson and Bilger*, 1992; *Hearn et al,* 2001]. However, fringing coral reefs typically have long, continuous stretches of reef of order several kilometers punctuated by narrow gaps of order hundreds of meters, while the limestone reefs off the Western Australian coast are more scattered and the gaps between the reefs are often considerably greater than the scale of the individual reefs. In coral reef systems wave setup behind the reef limits the cross reef flow, the magnitude of the setup depending on the wave forcing and cross sectional areas of the lagoon and gaps. Wave-driven flows over more isolated reefs have not been widely reported. *Mulligan et al* [2008] showed local wave forcing on a relatively small reef in the middle of a much larger bay affected circulation over a considerable fraction of the bay area. In a companion paper *Mulligan et al* [2010] used a numerical model to show radiation stress forcing due to wave breaking over the reef forced a strong current jet across the reef consistent with their observations. *Pattiaratchi et al* [1995] speculated the effects of waves may influence the circulation in the immediate vicinity of the reefs off Perth, though no observations were available to support this, and across the wider lagoon they conclude the effects of wave forcing could be neglected. Using the same data *Zaker et al* [2007] conclude the momentum balance in the lagoon is dominated by wind stress and bottom friction with a smaller but significant contribution from an alongshore pressure gradient. In contrast to these earlier studies this paper reports observations of wave-forced currents in the vicinity of the reefs off Perth and, during periods of large waves, the effects of wave forcing dominate and are felt across the lagoon several kilometers removed from the reefs.

The field site and instrument array are described in the next section followed by a description of the data obtained at each of the measurement sites. Model results using the hydrodynamic model XBeach are presented in the next section followed by discussion and conclusions.

2. FIELD SITE

Between July 2007 and May 2008 in situ measurements of waves, currents and water properties were made on and around a series of reefs off Perth, Western Australia. The field site is characterized by a series of shallow limestone reefs about 3km offshore and the depth over the top of the reefs varies between 1 to 4m. The bathymetry is shown in Figure 1 where the filled areas represent depths less than 4m showing the distribution of shallow reefs. Between the main reef line and the shore the mean depth is about 10m except at the northern end where a broad shallow region (<4m) extends from the outer reefs to the shore. The reef bathymetry is quite complex varying from reef pavement with roughness elements of order 10cm to bumps and holes in excess of 1m vertical extent over horizontal distances of a few meters. Between the reefs are areas of sand, seagrass and low relief reef pavement. Much of the reef is covered with kelp (Ecklonia Radiata) with a thallus length of order 1m which lie over to form a canopy of order 0.5m The field program consisted of in situ measurements of waves and currents at 11 sites shown in Figure 1 using a variety of point current meters, acoustic doppler current profilers (ADCP) and wave gauges. Bio-fouling is a major problem in these shallow waters and to ensure the highest quality data the array was deployed for approximately 6-8 weeks and then recovered to download data, replace batteries and clean sensors and mooring frames. The array was deployed four times during the course of the year. A summary of the deployment schedule and measured parameters used in this study is shown in Table 1. Additional data on water quality, temperature, salinity and nutrient distributions were also collected but are not reported here.

Nortek Vector Velocimeters (sites ADV1, ADV2, ADV3, and ADV4 in Figure 1) were deployed on the shoreward edge of the reefs in depths of 4-6m with Nortek Aquadopps (ADCPs) in the channels between the reefs (sites AQ1, AQ2 in Figure 1). MS1 was deployed inside the lagoon and was equipped with a Seabird SBE26 measuring waves and tides and an RDI ADCP measuring vertical profiles of mean currents. MS2 was deployed approximately 4km seawards of the reef line in 25m water depth and was equipped with a Seabird SBE26 measuring waves and tides. A Nortek AWAC with Acoustic Surface Tracking was deployed just seawards of the reef line (site AWAC in Figure 1) measuring wave height and direction and mean current profiles in 15m water depth. Finally two RDI ADCP's were deployed in the lagoon to the north and south of MS1 measuring mean current profiles at sites RDIN and RDIS in Figure 1.

An aim of the measurement program was to identify the role of waves and storm events in driving the circulation and exchange between the lagoon and offshore so, where possible, the instruments were set to resolve water motion associated with surface waves, requiring sampling rates of 1Hz or more. Table 2 summarises the instrument setup, including sampling rate, averaging times and interval and averaging . The Vectors were set to measure wave bursts of 2048 samples at 1Hz every 2 hours. The average of each wave burst (~34 minutes) gives a time series of mean currents at each of the ADV sites. Cell size in Table 2 refers to the size of the depth bins used in the ADCP profiles. During the first deployment a number of instruments were buried in sand to varying degrees, though only one (ADV4) was completely buried. On all subsequent deployments the moorings were deployed on reef or seagrass beds to avoid burial. The data return is shown in Table 1. In summary, no data are available at ADV4 for deployments 1 and 2 and at ADV1 for deployments 3 and 4. At ADV2 and ADV3 data from deployments 1 have not been used due to partial burial, and at ADV2 data from deployment 4 were also discarded because the sensor head became unaligned with the compass sometime during the deployment. The pressure data from all the ADV sites during deployment 1 appears to be good, the pressure sensor continuing to measure the wave induced pressure even after it was buried. Data from AQ1 for deployment one were also suspect due to partial burial, and the ADCP at MS1 failed in deployment one.

3. OBSERVATIONS

In addition to the observations at the sites described in the previous section a permanent directional wave buoy is maintained off Rottnest Island about 40 km south west of the field site at 32° 05' 39"S, 115° 24' 28" E in a depth of 48m (see Figure 1). Data from the wave buoy for the duration of the field program are shown in Figure 2. The study site is exposed to long period (T ~ 12s) Southern Ocean swell with maximum wave heights peaking at over 5m in winter. The biggest storm events occurred during the first deployment with a couple during the second and fourth deployments. As the waves propagate towards the coast the wave height is reduced due to refraction and partial shadowing from Rottnest Island. Linear regression between the root-mean-square wave heights at the AWAC (*Hrms(AWAC)*) and Rottnest Island (*Hrms(RI)*) gives

$$Hrms(AWAC) = .6Hrms(RI) \tag{1}$$

with a correlation r=0.93. A further reduction in root-mean-square wave height occurs between the AWAC and MS1 sites due to wave breaking over the reefs and bottom friction, the linear regression given by

$$Hrms(MS1) = .42Hrms(AWAC) \tag{2}$$

with r=0.95. In the remaining text, unless otherwise stated, *Hrms* refers to the root-mean-square wave height at the AWAC.

Previous studies in this region have concluded the nearshore alongshore currents are wind driven and the current speed is reasonably predicted using 2.5-3% of the wind speed [*Feng et al*, 2006; *Zaker et al*, 2007]. In Figure 3 the depth averaged alongshore currents at the AWAC from all four deployments are plotted against the alongshore wind. The alongshore currents are correlated with the alongshore wind, r=0.67, and the corresponding regression is given by,

$$V_c = -.01 + .01V_w \tag{3}$$

where V_c is the alongshore depth averaged current at the AWAC and V_w is the alongshore wind. Shoreward of the reef line at RDIS there is considerably more scatter between the depth averaged alongshore currents and the alongshore wind as shown in Figure 4. The grey and black points in Figure 4 correspond to times when *Hrms* is greater than 1.5 m and less than 1.5 m respectively. The strongest currents are towards the south when *Hrms* >1.5m, often occurring when the wind speed is small, and at times are opposed to the wind. After discarding data at times when *Hrms*>1.5m the correlation is 0.5 and the linear regression given by

$$V_c = .003 + .005V_w \tag{4}$$

where V_c is the depth averaged alongshore current at RDIS. Similarly, at RDIN the scatter between the depth averaged alongshore current and the alongshore wind is reduced by discarding data at times when *Hrms* >1.5m. In this case the correlation is 0.72 and the regression given by

$$V_c = .02 + .008V_w \tag{5}$$

where V_c is the depth averaged alongshore current at RDIN. Using (4) and (5) the wind driven component of the alongshore currents can be subtracted from the depth averaged alongshore currents at RDIS and RDIN respectively. The resulting residual currents at RDIN and RDIS are plotted against *Hrms* for all four deployments in Figure 5. The data have been binned in wave height and the residual currents averaged over each 0.2m bin and plotted as a solid line. The width of the shaded area is equal to one standard deviation and bins with less than 5 points are not included. During periods of low waves the curves are relatively flat but as *Hrms* increases the currents become more dependent on wave height, with northward currents at RDIN and southward at RDIS. During deployment 1 RDIN was recovered earlier than RDIS, missing a storm event during which time RDIS recorded some of the strongest southward currents.

ADCP's were located in channels between reefs at sites AQ1 and AQ2 shown in Figure 1. At these sites a wind driven component was present in both the alongshore and cross-shore currents and was subtracted using a linear regression derived using data from periods of low waves as above. The residual cross-shore flows are shown in Figure 6 plotted against *Hrms* at the AWAC. For low waves the curves are relatively flat but again the dependence on wave height becomes apparent under larger waves, in this case when *Hrms*>1m. At both sites offshore flows are associated with larger waves.

At the reef sites ADV1,…,4 there was little correlation with the cross-shore wind and we have not attempted to remove a wind forced component from the currents which are shown in Figure 7 plotted against *Hrms* at the AWAC. After discarding data, as discussed in the previous section, positive cross-reef currents (directed into the lagoon) are associated with larger waves at all the ADV sites. At sites ADV3 and ADV4 the cross-reef currents are reasonably well correlated with wave height, even under quite small waves at ADV3. At ADV1 the currents are weaker and only start to show a correlation with wave height when *Hrms* >2m. At ADV2 the currents are also weak but are correlated with wave height when *Hrms*>1m.

During periods of high waves we also observe an increase in sea level shoreward of the reef line relative to offshore. Shown in Figure 8 is the difference in sea level between MS1 and MS2 plotted against *Hrms* at the AWAC. A mean and trend were removed from MS1 and MS2 before differencing and while the resulting differences are small they are well within the specifications of the Seabird SBE26. With low waves the difference in sea level is about zero but as the wave height increases above about 1.5m the difference in sea level increases with wave height, with MS1 sea level being elevated relative to MS2.

As discussed in the introduction, to force significant mean flows across the reefs the waves must be big enough to break causing a cross-reef gradient in the radiation stress. A measure of depth-induced wave breaking is obtained by comparing root-mean-square wave height in front of the reefs (at the AWAC) with wave height at the back reef locations (at the ADV sites), as shown in 9. The root-mean-square wave heights at the ADV sites were calculated from the frequency spectra of bottom pressure, converted to surface wave height using linear wave theory. For low waves the root-mean-square wave heights are similar at the AWAC and ADV sites. However, as the offshore wave height increases we begin to see a reduction in wave height at the ADV sites relative to the AWAC. The point at which the ADV observations begin to diverge varies for the different sites; at ADV3 the data diverge when *Hrms*>0.5m at the AWAC, while the other sites begin to deviate when *Hrms*>1.5m. The reduction in wave height at the ADV sites can be attributed to wave breaking over the adjacent reefs. It is generally accepted that wave breaking is a depth dependent process and a simple rule of thumb for the inner surf zone is *Hrms*=.42*h*, where h is the water depth [*Thornton and Guza*, 1982]. Assuming the reef is shallow enough for the waves to break then the root mean square wave height behind the reefs at the ADV sites is governed by the depth over the corresponding reef crest. The onset of breaking at ADV3 at a lower wave height can be attributed to shallower water over the reef crest at ADV3 while deeper water over the reef at ADV1 limits the breaking to only the largest waves. The earlier onset of breaking at ADV3 also accounts for the correlation between cross-reef current and quite small waves at ADV3 shown in Figure 7. Further from the reefs at sites RDIS, RDIN and MS1, the effects of wave forcing do not become apparent until the wave height exceeds 1.5m. When *Hrms*<1.5m waves can propagate across some of the reefs without much breaking, for example at ADV1, and wave forcing and the corresponding circulation is likely to be confined to the immediate vicinity of the shallowest reefs where breaking still occurs.

4. MODELING

The numerical model XBeach was used to simulate the depth-averaged wave-driven circulation [*Roelvink et al*, 2009; *McCall et al,* 2010]. The wave field is obtained using a simplified time dependent wave action balance equation to give the directional distribution of the frequency integrated wave action density [*Holthuijsen et al*, 1989]. This time varying wave action balance includes refraction, shoaling, current refraction, bottom friction and wave breaking. The model forcing can accommodate non-stationary, time varying incident wave energy and the corresponding bound long wave [*van Dongeren et al*, 2003], but in this study the model has been run in stationary mode, forced at the offshore boundary with observed

Hrms, wave period and direction from the AWAC. The model domain is 269x440 cells and the grid size is 30x30 m. The wave model provides the spatial distribution of wave action, and therefore wave energy, which is then used to evaluate the radiation stress terms in the depth averaged, shallow water equations to obtain the mean flows. XBeach uses the Generalized Lagrangian Mean formulation (*Andrews and McIntrye*, 1978) where the momentum and continuity equations are expressed in terms of a Lagrangian velocity defined as the distance a water particle travels in one wave period, divided by that period. This Lagrangian velocity is equal to the sum of the mean Eulerian velocity and Stokes drift. Bottom friction is parameterized following *Federsen et al* (2000) calculated using the Eulerian velocity components and the magnitude of the wave induced velocity (*McCall et al*, 2010). To account for higher bottom roughness over the shallow reefs we introduced a depth dependent drag coefficient following *Daily and Harleman* [1966],

$$C_D = \frac{25g}{C^2} \tag{6}$$

where g is gravitational acceleration and C is given by,

$$C = \frac{h^\alpha}{0.02} \tag{7}$$

where h is the water depth and α=1/3. Introducing a spatially varying drag coefficient improved the model-data comparisons somewhat but clearly further improvements could be made in the formulation of frictional dissipation in complex reef environments and highly variable bottom roughness.

In the absence of wind, gradients in the radiation stress provide the primary forcing. While the direct forcing due to depth-induced wave breaking is confined to the relatively small and patchy reefs the effects on the circulation are seen across the model domain. In Figure 10 velocity vectors are plotted for the case where wave forcing at the offshore boundary is given by *Hrms*=2.2m, *T*=14s and direction=266° In the vicinity of the reefs the circulation is spatially variable with onshore flow over the reef crests (sites ADV1…4) and offshore flow in the channels (sites AQ1 and AQ2). At RDIS the flow is southward and at RDIN the flow is generally weaker and towards the northeast, all of which is in general agreement with the observations. The corresponding sea level is shown in Figure 11 where the lagoon setup is 10-12 cm. At MS1 the model setup is about 8cm compared with about 4 cm in the observations for the same wave height from Figure 8.

Qualitatively the model results are similar to the observations; a more quantitative assessment is made by comparing modeled and observed currents at the measurement sites. To investigate the wave-driven currents we focus on the high wave events, most of which occurred during deployment one. In Figure 12 model data comparisons during deployment 1 are shown at RDIS, RDIN, and AQ2 (data at other sites during deployment one are not usable for reasons discussed previously). The model was run for the period 22 July to 5 August, 2007 and includes several high wave events. The ADCP at RDIS was left in the water for considerably longer than the other instruments and captured a bigger wave event on 26-27 August. The squared correlation and corresponding p-value between model and data are shown in Table 3 together with the model skill defined by Warner et al (2005),

$$skill = 1 - \frac{\sum \left| X_{model} - X_{obs} \right|^2}{\sum \left(\left| X_{model} - \overline{X_{obs}} \right| + \left| X_{obs} - \overline{X_{obs}} \right| \right)^2} \qquad (8)$$

Perfect agreement between model and observations gives a skill of one while no agreement gives a skill of zero. The model does quite poorly predicting wave heights at MS1 during periods of low waves, being almost constant with offshore wave height though overall the squared correlation and skill are reasonably high. This might suggest the model wave height at MS1 is depth-limited due to too much breaking over the reefs, although attempts to reduce the breaking led to poorer model/data comparisons elsewhere. At RDIS the model and observed currents are in good agreement. At RDIN the model and observed currents are relatively weak but the model failed to capture the increase in currents associated with the larger waves on 30 July to 1 August and the model skill is low. At AQ2 the model tends to overestimate the offshore flow when the waves are low, but during the high wave event from 30 July to 1 August, the agreement is good. The strongest currents were observed at RDIS and AQ2 and at both sites the model agrees well with the observations with reasonable levels of skill.

Model data comparisons for the period October 17 to October 30 at three ADV sites (ADV1, ADV2, and ADV 3) and AQ1 are shown in Figure 13. At ADV3 the model does exceptionally well, but not so good at the other sites. At ADV2 there is very good correlation between model and data, but the model consistently overestimates the currents by about 0.1m/s as reflected in the lower skill value. This discrepancy remains unexplained.

5. DISCUSSION

The temperate reefs considered in this study are patchy, narrow with little or no reef flat, deep such that only larger waves break over them, and separated from land by a deep (~10m) and wide (~3km) lagoon. In comparison coral reefs are often more continuous, have wide reef flats, the reef crest is usually very shallow so that even small waves break, and the lagoons are often quite shallow. In both cases high dissipation over the reefs causes locally large gradients in radiation stress which can drive strong currents in the direction of wave propagation. Away from the reefs the dissipation is low such that the radiation stress gradients are no longer sufficient to drive the flow and, in the absence of any other forcing, continuity constraints cause the pressure field to adjust to accommodate the flow across the reefs. Analytic solutions reported by *Symonds et al* [1995] and *Gourlay* [1996a,b] show how the balance between the radiation stress gradients, pressure gradients and bottom friction vary with reef geometry and wave forcing over an idealized one dimensional reef. *Symonds et al* [1995] show the cross-reef transport increases as the width of the reef decreases, governed by,

$$R_2 = \frac{\text{Reef flat width}}{\text{Reef flat width} + \text{surf zone width}}. \qquad (9)$$

The reefs in this study correspond to the narrow reef limit, $R_2 \to 0$. In the literature the cause of the cross-reef current is sometimes attributed to wave setup [*Monismith*, 2007] estimated by assuming the radiation stress gradient through the surf zone is primarily balanced by the pressure gradient [*Tait*, 1972; *Hearn et al*, 2001]. On the 1D idealized reef described in Symonds et al (1995) the cross-shore flow approaches zero as $R_2 \to 1$ which, according to (9), corresponds to the case when the reef flat is wide compared with the width of the surf zone. The same limit is approached as the depth at the top of the reef slope becomes small compared to the depth at the breakpoint. In both these limiting cases the elevation at the top of the reef slope approaches the plane beach setup and the radiation stress gradient through the surf zone is balanced by the pressure gradient. However, in the narrow reef limit ($R_2 \to 0$) the cross-reef flow increases and the flow through the surf zone cannot be ignored.

In the two dimensional case the pressure field must also adjust to accommodate the alongshore flow [*Lowe et al*, 2009] as shown in Figure 11 where the north-south pressure gradient at the RDIS site is responsible for the observed southerly flow. Similarly a south-north pressure gradient drives a northerly flow at RDIN. Through this adjustment of the pressure field the effect of wave forcing due to depth-induced breaking over the very patchy reefs, with relatively small areal extent, is felt across the lagoon several kilometers removed from the reefs. To illustrate these dynamics XBeach is used to examine the relative magnitudes of the terms in the momentum balance. In the absence of rotation and surface wind stress the model equation for the depth-averaged and shortwave-averaged shallow water momentum in the x-direction (eastward) is given by

$$\underbrace{\frac{\partial u}{\partial t}}_{\substack{\text{local}\\\text{acceleration}}} \underbrace{+u\frac{\partial u}{\partial x}+v\frac{\partial u}{\partial y}}_{\text{advection}} = \underbrace{-\frac{F_x}{\rho h}}_{\substack{\text{radiation}\\\text{stress}}} \underbrace{-g\frac{\partial \zeta}{\partial x}}_{\substack{\text{pressure}\\\text{gradient}}} \underbrace{-\frac{\tau_{bx}}{\rho h}}_{\substack{\text{bottom}\\\text{friction}}} \underbrace{+\upsilon_h\left(\frac{\partial^2 u}{\partial x^2}+\frac{\partial^2 u}{\partial y^2}\right)}_{\substack{\text{horizontal}\\\text{friction}}} \tag{10}$$

where h is the water depth; u, v are the velocities in the x-direction (positive eastward) and y-direction (positive northward); τ_{bx} is the bed shear stress; F_x is the wave stresses; ζ is the sea surface elevation; ν_h is the horizontal eddy viscosity; g gravitational acceleration; ρ water density.

Time series of the dominant terms in the cross-shore (x-direction) momentum balance over the reef at ADV3 for 21 July to 4 August, 2007, are shown in Figure 14a where wave breaking provides a positive radiation stress gradient (solid grey line). The pressure gradient term (solid black line) is negative and opposes the radiation stress gradient (solid grey line). The resultant of the sum of the radiation stress gradient and the pressure gradient is shown by the dashed black line and produces a net force that drives a positive current in the direction of wave propagation and is balanced by negative bottom friction shown as the dashed grey line. In other words the radiation stress gradient due to wave breaking over the reef produces a force directed into the lagoon. Part of this force is balanced by the opposing pressure gradient and the remainder drives a current into the lagoon. The remaining terms in (10) are small and have not been plotted. At AQ2 the cross-shore momentum balance (Figure 14b) is dominated by the pressure gradient and bottom friction with some contribution from the advective terms (not plotted) reflected by the fact that the two dashed lines do not sum to zero. Radiation stress gradients are small because AQ2 is located in the channel between the reefs and there is no wave breaking. In this case the negative pressure gradient drives an offshore current as reflected in the positive bottom stress. At RDIS (Figure 14c) the alongshore (y-direction) momentum balance is dominated by the pressure gradient and bottom friction and the radiation stress gradient is small. In this case the negative pressure gradient drives a southward current as reflected in the opposing positive bottom friction and the remaining terms in (10) are small and have not been plotted.

The cross-reef variation of the dominant terms in the cross-reef momentum balance along a transect that crosses the reef at ADV2 is shown in Figure 15b. The corresponding *Hrms* and sea surface elevation are shown in Figure 15a and the bathymetry profile in Figure 15c. The wave height decreases rapidly through the surf zone across the reef crest with a corresponding increase in sea surface elevation (Figure 15a). Through the surf zone the positive radiation stress term provides an onshore directed force that is balanced in part by the negative pressure gradient term (Figure 15b). However, the excess radiation stress (i.e. the sum of the radiation stress gradient and pressure gradient) shown as the bold dashed line in Figure 15b drives a positive current into the lagoon and is balanced by bottom friction shown by the grey dashed line in Figure 15b.

Previous work reported by *Pattiaratchi et al* [1995] and *Zaker et al* [2002, 2007] for a region a few kilometers north of our study site concluded that wind forcing was dominant through most of the year. This might be explained by the even more patchy distribution of reefs in the region of the previous work. However, the previous researchers report spurious currents which at times are opposed to the wind and speculate that larger scale shelf features might be responsible. During periods of low waves we also see a dominance of wind forcing. However, we also observed spurious currents which are not obviously related to wind forcing but occur during high wave events and the strongest currents were observed during such events.

6. CONCLUSIONS

Previous work on wave-driven flows on reefs has focused on coral reefs where the areal extent of the reef is significant relative to the area of the neighboring lagoon. In contrast, temperate reefs often have a more patchy distribution and the areal extent of the reefs is small. Temperate reefs also have little or no reef flat compared to coral reef flats of several hundred meters. In situ measurements of waves and currents from a 12 month measurement program in a temperate reef system off Perth, Western Australia show primarily wind forced currents during periods of low waves. This result is consistent with *Zaker et al* [2002] from a study in a region just a few kilometers north of the current work. However, during high wave events currents in the vicinity of the reefs and at sites several kilometers removed from the reefs, are correlated with offshore wave height. During periods of high waves the observations showed onshore flow over the reefs, offshore flow between the reefs and alongshore flow in the lagoon behind the reefs. The strongest currents were observed during periods of high waves, sometimes with opposing, or light winds. Radiation stress gradients associated with wave breaking over the reefs provides the primary forcing and the pressure field adjusts to accommodate the flow where the waves are not breaking. Since the depth over the reef crests varies, the onset of breaking also varies from one reef to another. The numerical model XBeach was used to simulate the flow for two periods, 22 July to 5 August and 17-30 October, 2007. The model agreed qualitatively with observations with similar spatial variability in currents and elevated sea level in the lagoon. Comparison of observed and modeled time series of currents showed good quantitative agreement at some locations but at other locations the model failed to capture the stronger currents seen in the observations. Numerical results for the case when *Hrms*=2.2m revealed the high spatial variability in the currents in the vicinity of the reefs due to the spatial variability in forcing associated with wave breaking on the reefs. Examination of the dominant terms in the momentum balance showed that through the surf zone over the reef crest the radiation stress gradient opposes the pressure gradient. The cross-reef current is driven by the net force found by summing the radiation stress gradient and pressure gradient terms. In the lagoon behind the reefs radiation stress gradients were small and the flow governed by a balance between the pressure gradient and bottom friction.

ACKNOWLEDGEMENTS

The authors would like to thank the following for their invaluable support in all field operations; Stelios Kondylas, Jim Greenwood, James McLaughlin, Martin Lowrey, Ryan Downey, Andy Limbourne, Phil Adams, Ted Wassenberg, Ian McLeod and Quinton Dell. We would also like to thank Chaojiao Sun for her constructive comments and discussions, and Stephanie Contardo in preparing some of the figures. This work was supported with funding through the Western Australian Marine Science Institution.

REFERENCES

Andrews, D.G., and McIntrye, M.E., 1978, An exact theory of non-linear waves on a Lagragian-mean flow, *J. Fluid Mech.,* 89(4), 609-646.

Atkinson, M.J., and R.W. Bilger, (1992), Effects of water velocity on phosphate uptake in coral reef-flat communities, *Limnol. Oceanogr*., 37, 273-279.

Atkinson, M.J., E. Kotler, and P.Newton, (1994), Effects of water velocity on respiration, calcification and ammonium uptake of a porites compressa community, *Pacific Science*, 48, 296-303.

Bilger, R.W., and M.J. Atkinson, (1992), Anomalous mass transfer of phosphate on coral reef flats, *Limnol. Oceanogr.*, 37, 261-272.

Bowen, A.J., (1969), The generation of longshore currents on a plane beach, *J. Mar. Res.*, 27(2), 206-215.

Bowen,A.J., D.I. Inman, and V.P. Simmons, (1968), Wave set-down and set-up, *J. Geophys. Res.*, 73(8), 2569-2577.

Callaghan, D.P., P.Nielsen, N. Cartwright, M.R. Gourlay, and T.E. Baldock, (2006), Atoll lagoon flushing forced by waves, *Coastal Eng.*, 53, 691-704.

Daily, J.W., D.R.F. Harleman, (1966), Fluid Dynamics. Addison-Wesley, Reading, MA, pp. 297–298.

England, P.R., J. Phillips, J.R. Waring, G. Symonds, and R. Babcock, (2008), Modeling wave-induced disturbance in highly biodiverse marine macroalgal communities: support for the intermediate disturbance hypothesis, *Mar. Freshw. Res.*, 59, 515-520.

Feddersen, F., and Guza, R.T., (2000), Velocity moments in alongshore bottom stress parameterizations, *J. Geophys. Res.*, 105(C5), 8673-8686.

Feng, M., P. Craig, C. Fandry, J. Greenwood, N. Margvelashvili, A. Pearce, and G. Symonds, (2006), Physical Oceanography of the South Western Australian Shelf, pp 11-54. In: Keesing, J.K., Heine, J.N., Babcock, R.C., Craig, P.D., and Koslow, J.A.. Strategic Research Fund for the Marine Environment Final Report, Volume 2: the SRFME core projects 274p. Strategic Research Fund for the Marine Environment, CSIRO, Australia.

Gourlay, M.R., (1996a), Wave set-up on coral reefs. 1. Set-up and wave generated flow on an idealized two dimensional horizontal reef, *Coastal Eng.*, 27, 161-193.

Gourlay, M.R., (1996b), Wave set-up on coral reefs. 2. Set-up on reefs with various profiles, *Coastal Eng*., 28, 17-55.

Guza, R.T., and E.B Thornton, (1981), Wave set-up on a natural beach, *J. Geophys. Res*., 86(c5), 4133-4137.

Hearn, C.J., M.J. Atkinson, and J.L. Falter, (2001), A physical derivation of nutrient-uptake rates in coral reefs: effects of roughness and waves, *Coral Reefs*, doi 10.1007/s00338-001-0185-6.

Holthuijsen, L.H., N. Booij, and T.H.C. Herbers, (1989), A prediction model for stationary, short-crested waves in shallow water with ambient currents, *Coastal Eng.*, 13, 23-54.

Koslow, J. A., S. Pesant, M. Feng, A. Pearce, P. Fearns, T. Moore, R. Matear, and A. Waite, (2008), The effect of the Leeuwin Current on phytoplankton biomass and production off Southwestern Australia, *J. Geophys. Res.*, 113, C07050, doi:10.1029/2007JC004102.

Kraines, S.B., Yanagi, T., Isobe, M. and Komiyama, H.1998. Wind-wave-driven circulation on the Coral reef at Bora Bay, Miyako Island, Coral Reefs, 17, 133-143.

Kraines, S.B., A. Suzuki, T. Yanagi, M. Isobe, X. Guo, and H. Komiyama, (1999), Rapid water exchange between the lagoon and the open ocean at Majuro Atoll due to wind, waves and tide, *J. Geophys. Res*., 104(C7), 15,635-15,653.

Longuet-Higgins, M.S., (1970a), Longshore Currents Generated by Obliquely Incident Sea Waves, 1, *J. Geophys. Res*., 75(33), 6778-6789.

Longuet-Higgins, M.S., (1970b), Longshore Currents Generated by Obliquely Incident Sea Waves, 2, *J. Geophys. Res*., 75(33), 6790-6801.

Longuet-Higgins, M.S., and R.W. Stewart, (1964), Radiation stresses in water waves; a physical discussion, with applications, *Deep Sea Res*., 11, 529-562.

Lowe, R.J., J.L. Falter, S.G. Monismith, and M.J. Atkinson, (2009), Wave-driven circulation of a coastal reef-lagoon system, *J. Phys. Oceanogr*., 39, 873-893.

McCall, R.T., Van Thiel de Vries, J.S.M., Plant, N.G., Van Dongeren, A.R., Roelvink, J.A., Thompson, D.M., and Reniers, A.J.H.M, (2010), Two-dimensional time dependent hurricane overwash and erosion modeling at Santa Rosa Island, *Coastal Eng.*, 57, 668-683.

Monismith, S.G., (2007), Hydrodynamics of coral reefs, *Ann Rev. Fluid Mech*, 39, 37-55.

Mulligan, R.P., A.E. Hay, and A.J. Bowen, (2008), Wave-driven circulation in a coastal bay during the landfall of a hurricane, *J. Geophys. Res*., 113, C05026, doi: 10.1029/2007JC004500.

Mulligan, R.P., A.E. Hay, and A.J. Bowen, (2010), A wave-driven jet over a rocky shoal, *J. Geophys. Res.*, 115, C10038, doi:10.1029/2009JC006027.

Pattiaratchi, C., J. Imberger, N. Zaker, and T. Svenson, (1995), Perth Coastal Waters Study, Project P2: Physical Measurements, Centre for Water Research Report WP 958 CP, University of Western Australia.

Phillips, J.C., G.A. Kendrick, and P.S. Lavery, (1997), A test of a functional group approach to detecting shifts in macroalgal communities along a disturbance gradient, *Mar. Ecol. Prog. Ser*., 153, 125-138.

Roberts, H.H., and J.N. Suhayda, (1983), Wave-Current Interactions on a shallow reef (Nicaragua, Central America*), Coral Reefs*, 1, 209-214.

Roelvink, D., A. Reniers, A. Van Dongeren, Van Thiel de Vries, R. McCall, and J. Lescinski, (2009), Modeling storm impacts on beaches, dunes and barrier islands, *Coastal Eng*., 56, 133-1152.

Symonds,G., K.P. Black, and I.R. Young, (1995), Wave driven flow over shallow reefs, *J. Geophys. Res.*, 100(C2), 2639-2648.

Tait, R. J., (1972), Wave setup on coral reefs, *J. Geophys. Res*., 77, 2207-2211.

Tartinville, B., and J. Rancher, (2000), Wave induced flow over Mururoa Atoll reef, *J. Coastal Res*., 16(3), 776-781.

Thornton, E.B., and R.T. Guza, (1982), Energy saturation and phase speeds measured on a natural beach, *J. Geophys. Res.*, 87(c12), 9499-9508.

Thornton, E.B., and R.T. Guza, (1986), Surf Zone Longshore Currents and Random Waves: Field Data and Models, *J. Phys. Oceanogr*., 16,1165-1178.

Van Dongeren, A., A. Reniers, J. Battjes, and I. Svendsen, (2003) Numerical modeling of infragravity wave response during DELILAH, *J. Geophys. Res*., 108(C9), 3288 doi:10.1029/2002JC001332.

Warner, J.C., Geyer, W.R., and Lerczak, J.A., 2005, Numerical modeling of an estuary: A comprehensive skill assessment, *J. Geophys. Res.*, 110, C05001, doi:10.1029/2004JC002691.

Wernberg, T. and M.S. Thomsen, (2005), The effect of wave exposure on the morphology of Ecklonia radiata, *Aquatic Biology*, 83, 61-70.

Zaker, N.H., J. Imberger, and C. Pattiaratchi, (2002), Numerical simulation of a coastal boundary layer off Perth, Western Australia, *J. Coastal Res*., 18(3), 470-485.

Zaker, N.H., J. Imberger, and C. Pattiaratchi, (2007) Dynamics of the coastal boundary layer off Perth, Western Australia, *J. Coastal Res.*, 23(5), 1112-1130.

FIGURE CAPTIONS

Figure 1 Site location and instrument array. The contours are bathymetry and the filled light gray areas are where the shallow reefs are located with a water depth of less than 4m.

Figure 2 Rottnest swell wave and wind data. The grey shaded blocks mark the periods of the four deployments.

Figure 3 Depth averaged alongshore current (V_c) at the AWAC versus alongshore wind (V_w).

Figure 4 Depth averaged alongshore current (V_c) at RDIS versus alongshore wind (V_w). Black dots at times when *Hrms* <1.5m and grey dots when *Hrms* >1.5m.

Figure 5 Depth averaged alongshore current (V_c) minus the wind forced component (V_w) at RDIS (dark) and RDIN (light) plotted against *Hrms* at the AWAC for all four deployments.

Figure 6 Depth averaged cross-shore currents (U_c) minus wind forced component (U_w) at AQ1 and AQ2 plotted against *Hrms* at the AWAC for all deployments (except deployment 1 at AQ1).

Figure 7 Cross-shore currents at sites ADV1,…,4 plotted against *Hrms* at the AWAC; ADV1, deployments 1 and 2; ADV2, deployments 2 and 3; ADV3, deployments 1, 2 and 3; ADV4, deployments 3 and 4 only.

Figure 8 Difference in sea level $\delta\zeta$ between MS1 and MS2 (minus mean and trend), versus *Hrms* at the AWAC.

Figure 9 Root-mean-square wave heights at ADV1…4 versus *Hrms* at the AWAC for the four deployments.

Figure 10 Velocity vectors from XBeach in the vicinity of the reefs on July 22, 2007, with *Hrms*=2.2m, *T*=14s and direction=266°. The black crosses mark the instrument locations (see Figure 1).

Figure 11 Mean sea surface elevation from XBeach on July 22, 2007 with the same offshore wave forcing as Figure 10.

Figure 12 Model (circles and crosses) and observations (lines) from deployment one. (a) Significant wave height (Hsig) at the AWAC and MS1 sites, in bold and thin lines respectively. (b) Alongshore currents (V_c) at RDIN, RDIS and cross-shore currents (U_c) at AQ2.

Figure 13 Model (circles and crosses) and observations (lines) from deployment two. (a) Significant wave height (Hsig) at the AWAC and MS1 sites, in bold and thin lines respectively. (b) Cross-shore currents (U_c) at sites ADV1, ADV2, ADV3 and AQ1.

Figure 14 Time series of the dominant terms in the momentum balance. (a) cross-shore components of radiation stress gradient (solid grey), pressure gradient (solid black), bottom friction (dashed grey), and radiation stress gradient plus pressure gradient (dashed black) at

ADV3; (b) cross-shore components of the same terms at AQ2; (c) alongshore components of the same terms at RDIS.

Figure 15 Cross-reef transect near ADV2 of the dominant terms in the momentum balance for July 22, 2007 (same offshore wave forcing as Figure 10). (a) Hrms (solid) and sea surface elevation (dashed); (b) Radiation stress gradient (solid grey), pressure gradient (solid black), bottom friction (dashed grey) and radiation stress gradient plus pressure gradient (dashed black); (c) Bottom profile.

Table 1 Deployment schedule[1]

				Jul-07	Aug	Sep	Oct	Nov	Dec	Jan-08	Feb	Mar	Apr	May
Site	**Depth**	**Instr**	**Param**	**1 8 15 22 29**	**5 12 19 26**	**2 9 16 23 30**	**7 14 21 28**	**4 11 18 25**	**2 9 16 23 30**	**6 13 20 27**	**3 10 17 24**	**2 9 16 23 30**	**6 13 20 27**	**3 10 17 24 31**
MS1	8	SBE26	Pw,T											
		RDI ADCP	u,v,T,P											
MS2	25	SBE26	Pw,T											
RDIN	7	RDI ADCP	u,v,T,P											
RDIS	10	RDI ADCP	u,v,T,P											
AQ1	4	Aquadopp ADCP	u,v,T,P											
AQ2	8	Aquadopp ADCP	u,v,T,P											
ADV1	6	Vector	u,v,w, T,Pw											
ADV2	4	Vector	u,v,w, T,Pw											
ADV3	4	Vector	u,v,w, T,Pw											
ADV4	3.5	Vector	u,v,w, T,Pw											
AWAC	15.5	AWAC ADCP	ζ,u,v,P,T											

1 *u*,*v*,*w* horizontal and vertical velocity components, *T* temperature, *P* mean pressure, *Pw* wave resolving pressure, ζ sea surface elevation.

Table 2 Instrument and sampling parameters.

Site ID	Instrument	Sampling rate (Hz)	Burst length (s)	Measurement Interval (hours)	Cell size (m)
RDIN	RDI ADCP 300kHz	2	300	1	0.5
MS1	SBE26				
	Tides	4		0. 5	
	Waves	2	1200	6	
	RDI(600kHz)	2	300	1	0.5
RDIS	RDI ADCP 300kHz	2	300	1	0.5
MS2	SBE26				
	Tides	4		0.5	
	Waves	2	1200	6	
AQ1	Aquadopp 600kHz	6	1800	1	1
AQ2	Aquadopp 1MHz	6	600	1	0.5
ADV1	Vector	1	2048	2	
ADV2	Vector	1	2048	2	
ADV3	Vector	1	2048	2	
ADV4	Vector	1	2048	2	
AWAC	AWAC				
	Profile		600	1	0.5
	Waves	1	2048	2	

Table 3 Model/data correlations, corresponding p-values and skill at selected sites for deployments 1 and 2.

Deployment	Site	variable	r^2	p-value	skill
1	AWAC	Hrms	.92	0	1
1	MS1	Hrms	.64	.0003	.59
1	RDIN	V	.05	.43	.17
1	RDIS	V	.69	0	.77
1	AQ2	U	.5	.0033	.66
2	AWAC	Hrms	1	0	1
2	MS1	Hrms	.79	0	.59
2	ADV1	U	0	.83	.25
2	ADV2	U	.62	.0008	.4
2	ADV3	U	.85	0	.89
2	AQ1	U	.11	.25	.47

U and V are the cross-shore and alongshore velocity components respectively and Hrms the root mean square wave height.

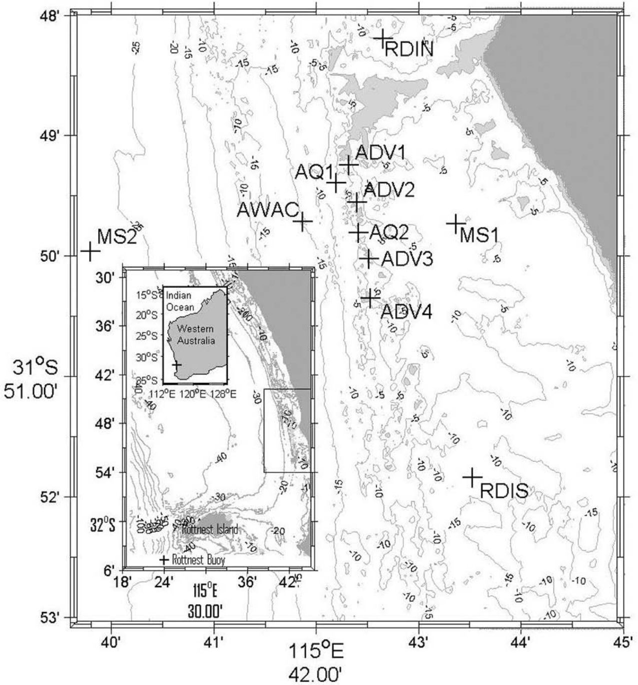

RDIN
ADV1
AQ1
ADV2
AWAC
AQ2
MS1
MS2
ADV3
ADV4
RDIS
Indian Ocean
Western Australia
Rottnest Island
Rottnest Buoy
31°S 51.00'
115°E 42.00'
115°E 30.00'
32°S

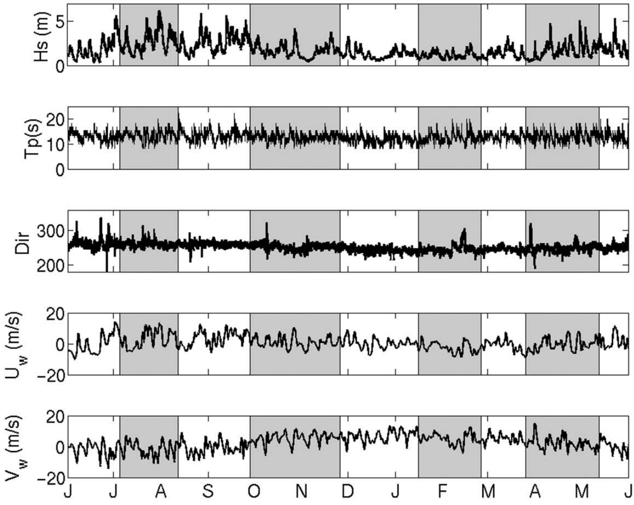
Hs (m)
Tp(s)
Dir
U_w (m/s)
V_w (m/s)
J J A S O N D J F M A M J

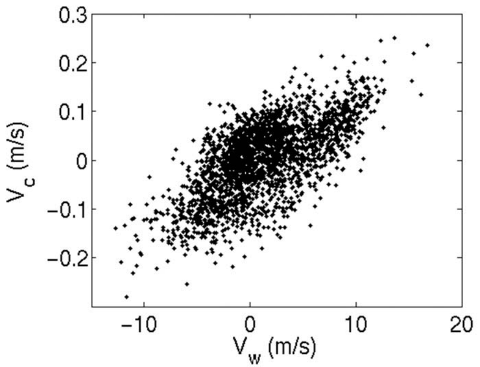
0.3
0.2
0.1
0
−0.1
−0.2
−10
0
10
20
V_c (m/s)
V_w (m/s)

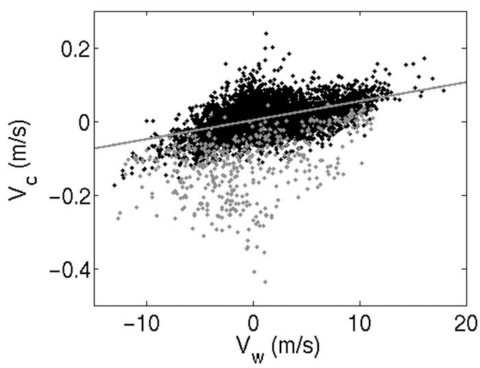

0.2
0
−0.2
−0.4
V_c (m/s)
−10
0
10
20
V_w (m/s)

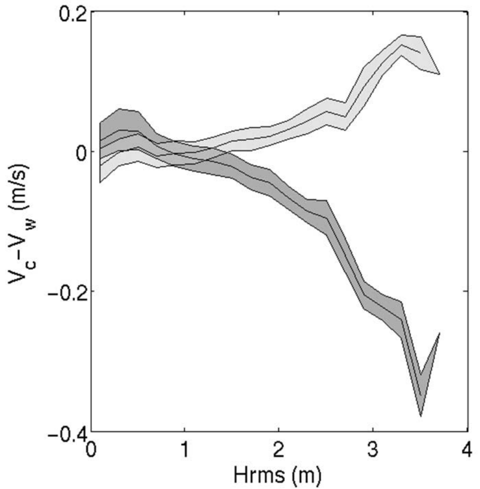

0.2
0
-0.2
-0.4
0
1
2
3
4
V_c-V_w (m/s)
Hrms (m)

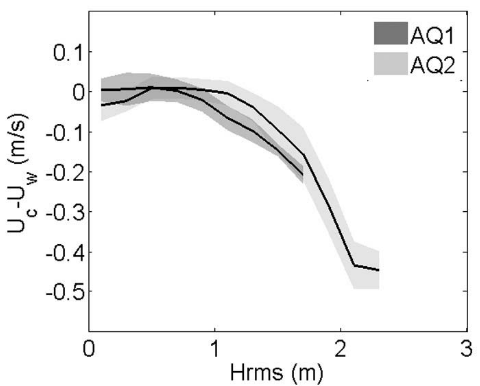

AQ1
AQ2
0.1
0
-0.1
-0.2
-0.3
-0.4
-0.5
$U_c - U_w$ (m/s)
0
1
2
3
Hrms (m)

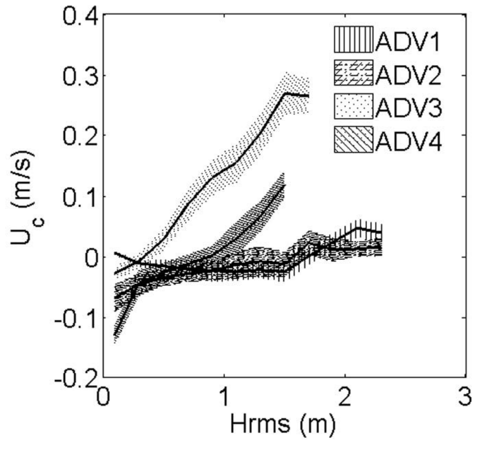

ADV1
ADV2
ADV3
ADV4
U
c
(m/s)
Hrms (m)
0.4
0.3
0.2
0.1
0
-0.1
-0.2
0
1
2
3

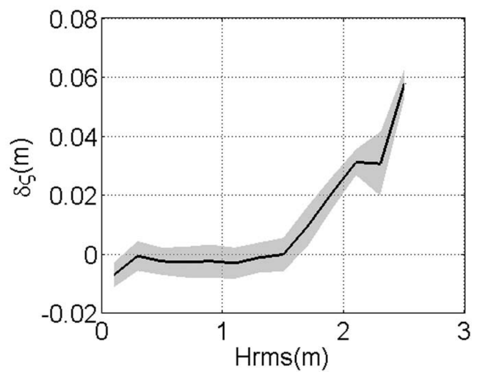

0.08
0.06
0.04
0.02
0
-0.02
δς(m)
0
1
2
3
Hrms(m)

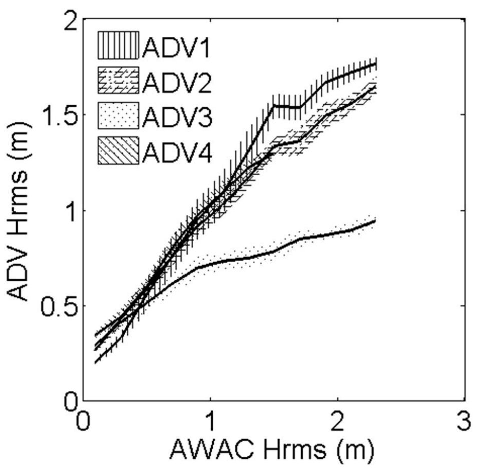
ADV1
ADV2
ADV3
ADV4
ADV Hrms (m)
AWAC Hrms (m)
0
0.5
1
1.5
2
0
1
2
3

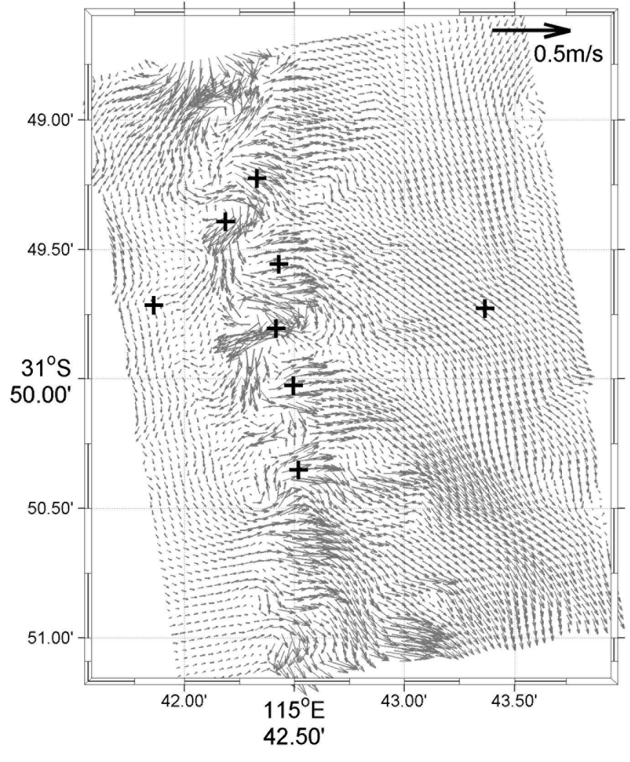

0.5m/s
49.00'
49.50'
31°S
50.00'
50.50'
51.00'
42.00'
115°E
42.50'
43.00'
43.50'

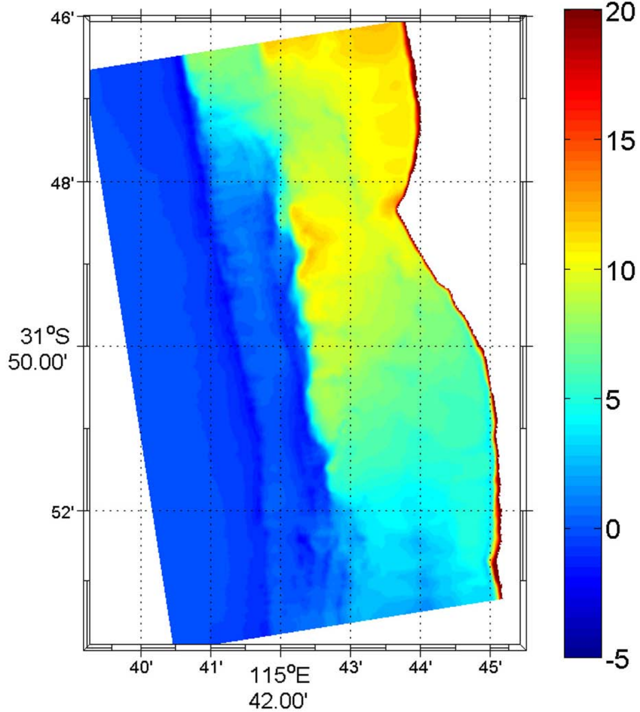
46'
48'
31°S
50.00'
52'
40'
41'
115°E
42.00'
43'
44'
45'
20
15
10
5
0
-5

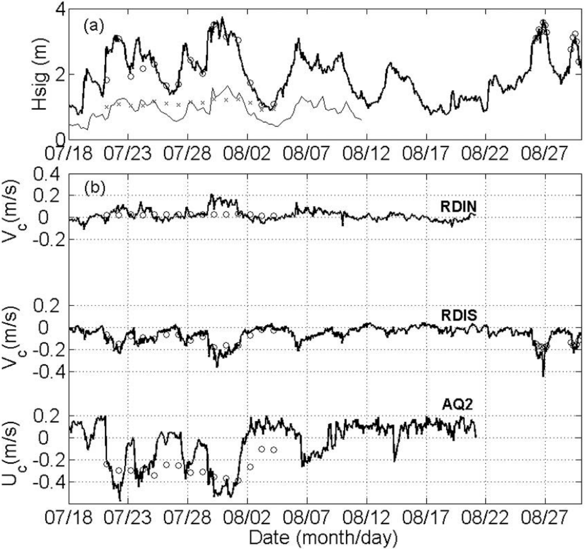

(a)
Hsig (m)
4
2
0
07/18
07/23
07/28
08/02
08/07
08/12
08/17
08/22
08/27
(b)
0.4
0.2
0
-0.2
V_c(m/s)
RDIN
RDIS
-0.4
AQ2
U_c(m/s)
Date (month/day)

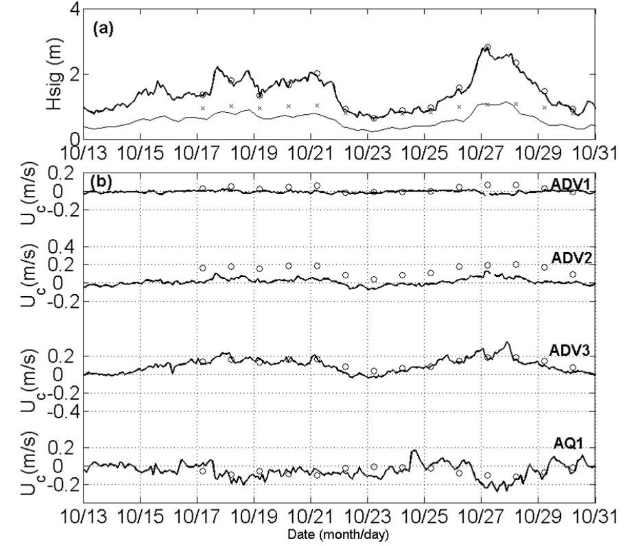

(a)
Hsig (m)
4
2
0
10/13
10/15
10/17
10/19
10/21
10/23
10/25
10/27
10/29
10/31
(b)
ADV1
ADV2
ADV3
AQ1
U_c (m/s)
0.4
0.2
0
-0.2
-0.4
Date (month/day)

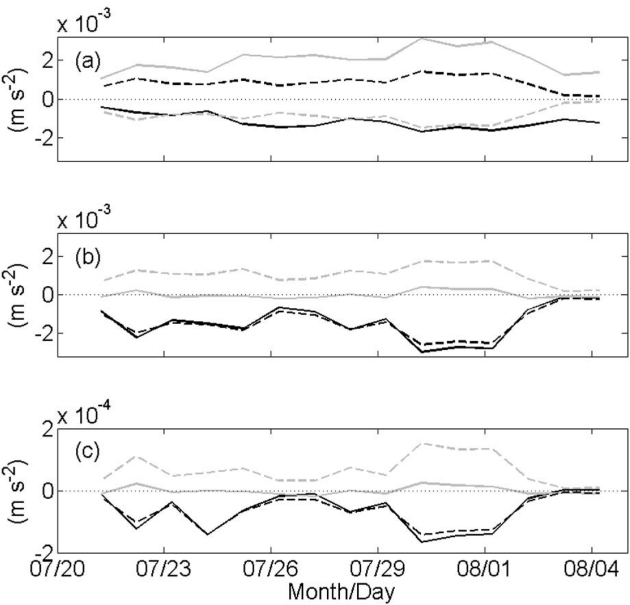
x 10^-3
(a)
(m s^-2)
2
0
-2
x 10^-3
(b)
(m s^-2)
2
0
-2
x 10^-4
(c)
(m s^-2)
2
0
-2
07/20
07/23
07/26
07/29
08/01
08/04
Month/Day

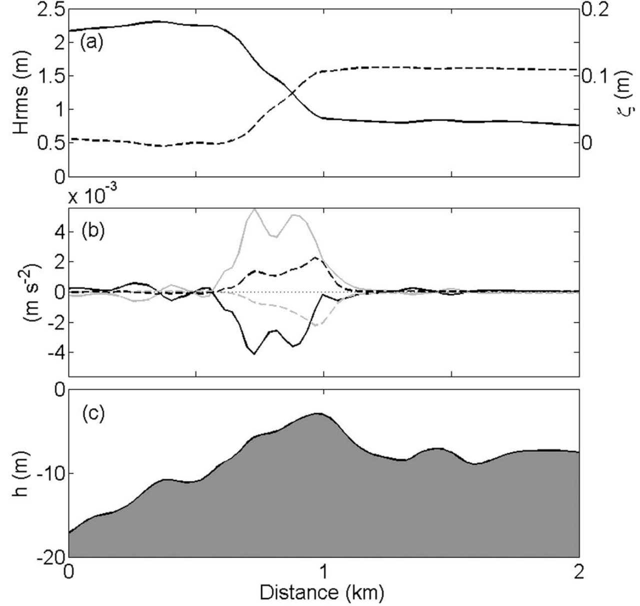

(a)
Hrms (m)
ξ (m)
2.5
2
1.5
1
0.5
0
0.2
0.1
0
x 10^-3
(b)
(m s^-2)
4
2
0
-2
-4
(c)
h (m)
0
-10
-20
0
1
2
Distance (km)